Cellular/Molecular

Membrane Potential Changes in Dendritic Spines during Action Potentials and Synaptic Input

Lucy M. Palmer and Greg J. Stuart
Division of Neuroscience, John Curtin School of Medical Research, Australian National University, Canberra, Australian Capital Territory 0200, Australia

Excitatory input onto many neurons in the brain occurs onto specialized projections called dendritic spines. Despite their potential importance in neuronal function, direct experimental evidence on electrical signaling in dendritic spines is lacking as their small size makes them inaccessible to standard electrophysiological techniques. Here, we investigate electrical signaling in dendritic spines using voltage-sensitive dye imaging in cortical pyramidal neurons during backpropagating action potentials and synaptic input. Backpropagating action potentials were found to fully invade dendritic spines without voltage loss. The voltage change in dendritic spines during synaptic input ranged from a few millivolts up to ~20 mV. During hyperpolarization of the membrane potential, the amplitude of the synaptic voltage in spines was increased, consistent with the expected change resulting from the increased driving force. This observation suggests that voltage-activated channels do not significantly boost the voltage response in dendritic spines during synaptic input. Finally, we used simulations of our experimental observations in morphologically realistic models to estimate spine neck resistance. These simulations indicated that spine neck resistance ranges up to ~500 MΩ. Spine neck resistances of this magnitude reduce somatic EPSPs by <15%, indicating that the spine neck is unlikely to act as a physical device to significantly modify synaptic strength.

Introduction

Ever since their discovery by Santiago Ramón y Cajal more than a century ago, dendritic spines have fascinated neuroscientists. Because the vast majority of excitatory synaptic input in many brain regions is made directly onto dendritic spines, understanding spine physiology and function is critical to understanding synaptic transmission. Previous experimental work on signaling in dendritic spines is based primarily on measurements of changes in intracellular ion concentrations during action potentials (APs) and synaptic input (Muller and Connor, 1991; Yuste and Denk, 1995; Rose et al., 1999; Sabatini and Svoboda, 2000; Rose and Konnerth, 2001; Sabatini et al., 2002). These studies indicate that spines are invaded by backpropagating APs (bAPs) and can act as biochemical compartments during synaptic input (Muller and Connor, 1991; Yuste and Denk, 1995; Sabatini and Svoboda, 2000), both of which are believed to be important for the induction of some forms of synaptic plasticity (Kampa et al., 2007; Sjöström et al., 2008). In addition, theoretical studies show that differences in spine neck resistance may serve as a mechanism to modulate synaptic strength (Koch and Poggio, 1983; Koch and Zador, 1993). Other theoretical work indicates that synaptic input onto dendritic spines may be amplified by voltage-activated channels (Miller et al., 1985; Perkel and Perkel, 1985; Segev and Rall, 1988), with recent experimental evidence supporting this idea (Araya et al., 2007) (but see Bloodgood and Sabatini, 2005).

Although it is clear that spines can act as biochemical compartments (Muller and Connor, 1991; Yuste and Denk, 1995), the extent to which they compartmentalize electrical signals is unknown. Here, we address this gap in knowledge through the use of voltage-sensitive dye imaging from dendritic spines on basal dendrites of cortical pyramidal neurons. This technique enables us to measure electrical signals in neuronal structures that are inaccessible to direct electrophysiological recordings. We show that bAPs invade dendritic spines without voltage loss. During synaptic input, we find that while there was evidence for electrical compartmentalization in some spines (Denk et al., 1995), the synaptic voltage response in the majority of dendritic spines is small. Furthermore, based on changes in the amplitude of synaptic responses in dendritic spines during membrane hyperpolarization, we conclude that these responses are not significantly amplified by voltage-activated channels. Simulation of our experimental findings in morphologically realistic models indicates that spine neck resistance ranges up to ~500 MΩ, in agreement with previous estimates from electron microscopy (Harris and Stevens, 1989), diffusion measurements (Svoboda et al., 1996; Bloodgood and Sabatini, 2005), and recent modeling based on calcium imaging data (Grunditz et al., 2008). Spine neck resistances of this magnitude reduce the amplitude of somatic EPSPs by <15%, indicating that spine neck is unlikely to act as a physical device to modulate synaptic strength.

Materials and Methods

Preparation. Wistar rats (3–5 weeks of age) were anesthetized by inhalation of halothane and decapitated according to guidelines approved by the Animal Experimentation Ethics Committee of the Australian National University. Brain slices of somatosensory cortex (300 μm thick) were prepared using a vibrating tissue slicer and perfused with oxygenated (95% O_2/5% CO_2) extracellular solution [artificial CSF (ACSF)] containing 125 mM NaCl, 25 mM $NaHCO_3$, 25 mM glucose, 3 mM KCl,

Received Dec. 9, 2008; revised April 9, 2009; accepted April 15, 2009.

We thank Arnd Roth, Michael Häusser, Maarten Kole, Clarke Raymond, and Steve Redman for discussions and comments on previous versions of this manuscript.

Correspondence should be addressed to Greg J. Stuart at the above address. E-mail: greg.stuart@anu.edu.au.

DOI:10.1523/JNEUROSCI.5847-08.2009

 0270-6474/09/296897-07$15.00/0

1.25 mM NaH_2PO_4, 2 mM $CaCl_2$, 1 mM $MgCl_2$, pH 7.4. Slices were incubated at 35°C for 30 min and subsequently maintained at room temperature (~22°C). During recording, slices were bathed in ACSF that usually contained high calcium (3 mM $CaCl_2$; $n = 56/70$), and in some cases also low magnesium (100 μM; $n = 4/70$) for synaptic stimulation experiments. Since there was no difference in synaptic responses in the different conditions data were pooled. All recordings were made at room temperature.

Somatic whole-cell recordings were made from visually identified layer 5 pyramidal neurons using infrared differential interference contrast (DIC) optics (Stuart et al., 1993). Whole-cell recording pipettes (7–10 MΩ) were tip-filled with intracellular solution containing 135 mM K-gluconate, 7 mM NaCl, 10 mM HEPES, 2 mM $MgCl_2$, 2 mM Na_2-ATP, and 0.3 mM Na_2-GTP (pH 7.2 adjusted with KOH). Pipettes were backfilled with intracellular solution containing 3 mg/ml voltage-sensitive dye JPW3028 (synthesized and provided by J. P. Wuskell and L. M. Loew, University of Connecticut, Farmington, CT). Whole-cell recordings were maintained for 45–60 min to allow for the passive transfer of dye into the neuron before the patch pipette was removed. The dye-filled neuron was left undisturbed for up to 2 h before being repatched. All recordings were made using a current-clamp amplifier (BVC-700; Dagan). Voltage was filtered at 10 kHz and digitized at 50 kHz using an ITC-16 interface (InstruTech). AxoGraph software was used for both acquisition and analysis.

Confocal imaging. Voltage-sensitive dye fluorescence changes were detected with a confocal microscope (FV300, Olympus) with a 60× objective (Olympus; numerical aperture, 0.9) using an open pinhole. Neuronal morphology could readily be visualized because of the high resting fluorescence of voltage-sensitive dyes. Basal dendrites were identified, and large (~1 μm in length) spines located 37–140 μm from the soma were selected using frame-scans. A line-scan (~20 pixels per micron spatial resolution) was positioned to transverse the spine of interest and parent dendrite. Fluorescence signals were recorded at ~800 Hz. To determine the impact of sampling at 800 Hz on the amplitude of fast voltage changes, we decimated APs and simulated EPSPs in spines (obtained from our morphologically realistic model–see below) to obtain an effective sampling rate of 800 Hz. This analysis indicated that filtering resulting from sampling at 800 Hz will underestimate the peak amplitude of bAPs by <20% and synaptic responses in spines by between 8 and 15%, depending on the spine neck resistance (data not shown). During voltage imaging, excitation was performed with a 543 nm laser (HeNe; Melles Griot) limited to <150 ms per trial. To increase signal-to-noise we typically averaged >120 responses per spine. AP amplitude and spine morphology were continuously monitored throughout experiments, and the experiment was stopped if either changed significantly (control AP: 101.0 ± 2.1 mV compared with 99.5 ± 2.4 mV at the end of the experiment; $p > 0.05$; $n = 13$). During synaptic stimulation, a patch pipette filled with extracellular solution and 100 μM Alexa Fluor 543 for visualization was placed within 10 μm of the spine of interest. To ensure that we were recording from spines that received direct synaptic input, neurons were repatched with pipettes filled with the calcium-sensitive dye Oregon Green BAPTA 1 (200 μM; Invitrogen), and before voltage imaging, calcium transients (excitation: 488 nm laser; Melles Griot) in response to synaptic stimulation were recorded at the resting membrane potential. Voltage imaging was only performed if the calcium signal in the spine head was highly localized and the synapse had a high probably of release (typically >0.8). When tested, fluorescent signals generated by synaptic input were blocked by the AMPA receptor antagonist DNQX (10 μM, $n = 3$) (data not shown). The probability of release was determined for each spine before voltage imaging based on the number of trails with clear calcium transients (successes) divided by the total number of trails (supplemental Fig. 1*A*,*B*, available at www.jneurosci.org as supplemental material). Synaptic responses were interleaved (0.3 Hz) with somatically evoked APs and the resulting fluorescence signal was recorded for *post hoc* analysis. In some experiments, hyperpolarizing pulses generated by somatic current injection (150 ms, ~300–400 pA) were interleaved with somatically evoked APs, and the resulting spine and dendrite fluorescence were recorded without or with concurrent synaptic stimulation. The stability of synaptic stimulation was analyzed by comparing voltage responses in spines during the first half of trials with that during the second half of trials. Photo bleaching was assessed by investigating the amplitude of bAP signals in spines, and did not significantly differ during the course of any of the experiments (first half of trials: 6.0 ± 0.5% $\Delta F/F$; second half of trials: 6.1 ± 0.6% $\Delta F/F$; $p > 0.05$; $n = 13$, data where there was a clear synaptic spine response at rest).

Analysis. To remove problems caused by trial-to-trial temporal jitter, individual APs were aligned to the voltage recorded via the somatic recording pipette, and synaptically evoked signals were aligned to the stimulus artifact. Signals were considered to have a clear response at rest if their peak amplitude was >2.5 times the SD of the noise. The amplitude of optical signals was expressed as the percentage change in light intensity divided by the resting light intensity ($\Delta F/F$), and response rise times (10–90%) and width at half amplitude were also measured. Due to the small signal-to-noise ratio, where stated the averaged responses from individual spines were summed together to create a superaverage. All distances were determined from confocal image stacks using ImageJ software. Membrane potential values were corrected for a 12 mV junction potential. Pooled data are presented as mean ± SEM. Statistical tests used a Student's *t* test or ANOVA at a level of significance of 0.05. All fluorescence signals were filtered at 200 Hz for display purposes only.

Modeling. Simulations were performed with NEURON (Hines and Carnevale, 1997) using a morphologically realistic model of a cortical layer 5 pyramidal neuron (Stuart and Spruston, 1998). The passive electrical properties R_m, C_m, and R_i were set to 17,000 Ωcm^2, 1 μF/cm^2 and 105 Ωcm, respectively, based on recently published experimental data for basal dendrites of these neurons (Nevian et al., 2007). R_m was halved and C_m doubled in spiny compartments. In addition, we explicitly modeled a spine with a head diameter and neck length of 1 μm placed on a basal dendrite 80 μm from the soma. Spine neck resistance was varied by changing spine neck diameter over a range from 0.23 to 0.051 μm (neck resistance 25 to ~500 MΩ), or from 0.4 to 0.004 μm (neck resistance 10 MΩ to 84 GΩ) (supplemental Fig. 2, available at www.jneurosci.org as supplemental material). Steady-state attenuation from the soma to the base of the simulated spine located 80 μm from the soma was 5% (see supplemental Fig. 2, available at www.jneurosci.org as supplemental material). "AMPA" EPSPs were simulated using a synaptic conductance of 500 pS (Bekkers and Stevens, 1990) with an exponential rise and decay with time constants of 0.2 and 2 ms, respectively (Häusser and Roth, 1997). This led to local dendritic EPSP amplitudes of ~1.5 mV at the dendritic location of the spines in our study, consistent with recent experimental observations (Nevian et al., 2007). EPSPs were placed on the spine head or the adjacent parent dendrite, and the voltage response measured either in the spine head, the parent dendritic shaft, or at the soma. To mimic activation of neighboring spines other than the one that was imaged, we placed additional synaptic inputs onto the same dendrite as that with the reconstructed spine. The number of additional inputs on the same dendrite was adjusted to match the amplitude of the "background" depolarization observed in experimental responses in spines and the adjacent dendrite. Resting membrane potential in the model was set to −75 mV.

Results

Voltage imaging in dendritic spines

Dendritic spines receive two main electrical signals: the voltage associated with excitatory synaptic input (EPSPs) and that mediated by active dendritic events such as bAPs. The interaction of these two events is thought to be important for the induction of some forms of synaptic plasticity (Magee and Johnston, 1997; Markram et al., 1997; Koester and Sakmann, 1998). To investigate electrical signaling in dendritic spines, we used fluorescent voltage imaging (Stuart and Palmer, 2006). These experiments were performed on spines located on average 80 ± 2 μm (range: 37–140 μm; $n = 106$) from the soma on basal dendrites of cortical layer 5 pyramidal neurons filled with voltage-sensitive dye and imaged with a confocal microscope. Because of the high resting fluorescence of voltage-sensitive dyes, neuronal morphology including spines could be readily visualized (Fig. 1*A*,*B*).

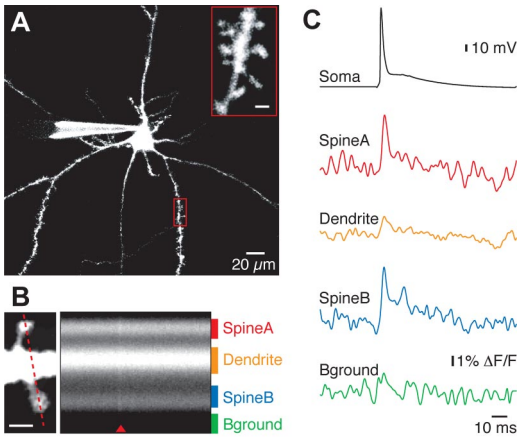

Figure 1. Imaging membrane potential in dendritic spines. ***A***, Image of a layer 5 pyramidal neuron filled with voltage-sensitive dye. Magnification of boxed region illustrates dendritic branch with spines (inset; scale bar, 1 μm). ***B***, Image of spines on a basal dendrite (left; 68 μm from the soma) showing a line-scan (dashed red line; scale bar, 1 μm) transversing two spines and the resulting average fluorescence change in response to ~100 bAPs (right). Red arrowhead indicates timing of stimulus, and colored bars represent the labeled regions of interest. ***C***, Fluorescence traces (colored) in response to somatically evoked bAPs (black) for the regions of interest shown in ***B***. Note that the background signal is negligible, illustrating high spatial resolution.

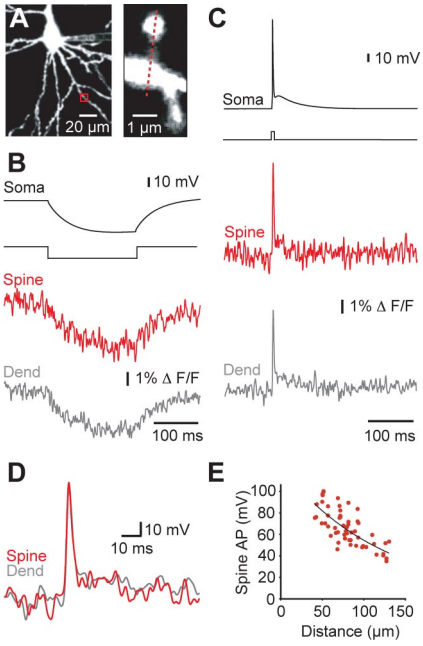

Figure 2. bAPs successfully invade spines. ***A***, Layer 5 pyramidal neuron filled with voltage sensitive dye (left) and magnified view of the region outlined by the box (red) showing the line-scan (dashed line) transversing a spine and its parent dendrite (right) located 94 μm from the soma. ***B***, Hyperpolarization recorded at the soma (black) in response to somatic current injection (~−300 pA; 150 ms; second from the top), and corresponding changes in fluorescence recorded in the spine (red) and parent dendrite (gray) shown in ***A***. Exponential curves were fitted to the fluorescence traces, and amplitudes were calculated at steady state (120–150 ms; average of 160 trails). ***C***, Fluorescence change recorded in the spine (red) and parent dendrite (gray) shown in ***A*** in response to somatically evoked APs (black; average of ~150 individually aligned trials; 2 ms somatic current pulse; second from the top). ***D***, Comparison of bAP fluorescence in the spine (red) and dendrite (gray) after normalization and conversion to absolute voltage based on the hyperpolarization response at each location (assuming 5% steady-state voltage attenuation from the soma to the spine). ***E***, Plot of bAP amplitude in basal dendrites at different distances from the soma. The data are fitted with a single exponential, which is used in subsequent experiments to convert spine and parent dendrite fluorescent signals into absolute voltage during synaptic input.

Backpropagating action potentials invade spines without voltage loss

We first investigated how effectively bAPs invade dendritic spines. APs in these experiments were generated by somatic current injection, and changes in fluorescence were measured using line-scans (~800 Hz) positioned to transverse the spine of interest and parent dendrite (Fig. 1*B*). The absence of a significant background signal in regions just adjacent to imaged spines indicated that the spatial resolution of our recording system is sufficient to detect voltage-dependent fluorescent changes isolated to dendritic spines and parent dendrites during APs (Fig. 1*C*).

Direct comparison of the magnitude of the fluorescence signal in the spine and dendrite is not possible because voltage-sensitive dyes bind not only to the plasma membrane but also to internal membranes that do not undergo a change in membrane potential during electrical signaling. Fluorescence signals in spines and parent dendrites were therefore normalized to a signal of known amplitude (Djurisic et al., 2004). In our case, we used the fluorescence change generated by hyperpolarizing steady-state somatic current injections (Fig. 2*A*,*B*) to normalize fluorescent signals in the spine and parent dendrite during bAPs (Fig. 2*C*). This approach is valid as steady-state voltage changes in the spine and parent dendrite are effectively identical unless the spine neck resistance is extremely high ($>$ 10 GΩ) (see supplemental Fig. 2, available at www.jneurosci.org as supplemental material). Previous estimates predict spike neck resistance is significantly lower than this by more than an order of magnitude (Harris and Stevens, 1989; Svoboda et al., 1996; Bloodgood and Sabatini, 2005; Grunditz et al., 2008). Normalized bAP fluorescence signals were then converted to absolute voltage (Fig. 2*D*) based on the amplitude of the somatic response to steady-state current injection, assuming 5% steady-state voltage attenuation from the soma to the average location of dendritic spines in our study (80 μm from the soma) (supplemental Fig. 2, available at www.jneurosci.org as supplemental material).

This analysis indicated that the average amplitude of bAPs in the spine and parent dendrite was essentially identical (66.4 $\pm$ 2.2 and 66.7 $\pm$ 3.2 mV, respectively; $n = 55$), illustrating that bAPs successfully invade dendritic spines without voltage attenuation. These results are in agreement with a study using second harmonic imaging (Nuriya et al., 2006). Consistent with the absence of voltage attenuation of bAPs as they invade dendritic spines, there was no significant difference in the half-width of bAPs in the spine and parent dendrite (spine: 3.08 $\pm$ 0.28 compared with dendrite: 2.90 $\pm$ 0.21 ms; $p > 0.05$, $n = 55$). The calculated bAP voltage in the spine and dendrite was smaller at more distal dendritic locations (Fig. 2*E*), consistent with the recently reported attenuation of bAPs in basal dendrites of layer 5 pyramidal neurons, based on direct patch-clamp recordings (Nevian et al., 2007).

Dendritic spine voltage in response to synaptic input

Dendritic spines are the main site of excitatory synaptic input in many neuronal types; however, the voltage response in spines during synaptic input and the role of spines in shaping this voltage change are unknown. To address this we performed voltage imaging in spines receiving synaptic input. Neurons were filled with a calcium indicator as well as voltage-sensitive dye, and synaptic responses were evoked by placing an extracellular stimulating pipette in close proximity (within 10 μm) to the spine of interest (Fig. 3*A*). Calcium imaging was used to localize active

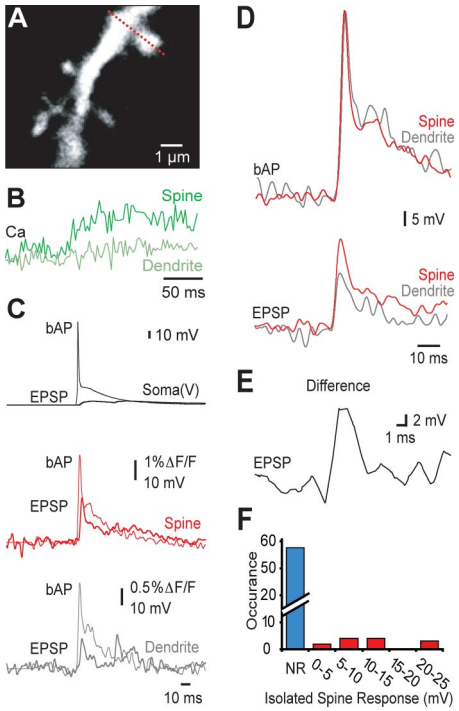

Figure 3. Voltage response in dendritic spines during synaptic input. ***A***, Basal dendrite from a layer 5 pyramidal neuron filled with voltage-sensitive dye showing the location of a line-scan (dashed line) transversing a spine located 73 μm from the soma. ***B***, Calcium transients recorded in the spine (dark green) and parent dendrite (light green) shown in ***A***. ***C***, Average somatic whole-cell voltage (black, top) and the corresponding fluorescence responses for active spines (red, middle) and parent dendrites (gray, bottom) during somatic bAPs (thin traces) and synaptic input (thick traces) ($n = 13$). Synaptic fluorescence signals in the spine (red) and dendrite (gray) were converted to voltage using the calculated amplitude of the bAP (from the calibration curve in Fig. 2*E*). ***D***, Direct comparison of the average response from all spines with a measurable synaptic fluorescence ($n = 13$) illustrating the spine (red) and dendrite (gray) voltage change during bAPs (top) and synaptic input (bottom). ***E***, The active spine response was obtained by subtracting the parent dendrite response from the active spine response. This isolated active spine response was on average 13 mV ($n = 13$). ***F***, Histogram of the amplitude of isolated spine responses (obtained after subtraction of the dendritic response) for all spines. Spines with a clear response at the resting membrane potentials are indicated in red. "NR" indicates no detectable response at the resting membrane potential (blue).

spines (Fig. 3*B*) and voltage imaging was only performed on spines where an isolated calcium signal was detected during synaptic stimulation (supplemental Fig. 1, available at www.jneurosci.org as supplemental material) (typical spine/dendrite $\Delta F/F > 2$). We estimated the probability of release based on the failure rate of spine calcium transients and selected spines where the probability of release was high (on average 0.87 ± 0.05) (supplemental Fig. 1, available at www.jneurosci.org as supplemental material). We next recorded voltage fluorescence signals in response to bAPs and synaptic input in active spines and the parent dendrite (Fig. 3*C*). We focused on spines where there was a clear synaptic response at the resting membrane potential, and used the amplitude of the fluorescent change during the bAP at each dendritic location (see Fig. 2*E*) to convert synaptic fluorescence responses in the spine and adjacent dendrite into millivolts (Fig. 3*D*) ($n = 13$). Similar results were obtained when synaptic fluorescence signals were converted to millivolts based on the amplitude of the somatic steady-state response (data not shown). The stability of synaptic stimulation in these spines was judged to be stable based on a comparison of the voltage responses in spines during the first half of trials (0.61 ± 0.06% $\Delta F/F$) with that during the second half of trials (0.55 ± 0.06% $\Delta F/F$; $p > 0.05$; $n = 13$) (supplemental Fig. 3, available at www.jneurosci.org as supplemental material).

Although care was taken to use minimal stimulation, we predict that multiple synaptic inputs were activated in these experiments as the average somatic EPSP amplitude was 5.3 ± 0.6 mV ($n = 13$). Background depolarization from inputs other than the activated spine will sum with the fluorescent response recorded in the spine and dendrite. To isolate the synaptic voltage response in the spine, we therefore subtracted the response in the parent dendrite from the spine response. After this procedure, the amplitude of the isolated spine response during synaptic stimulation ranged from 0 to 25 mV and was on average 11.1 ± 2.7 mV (Fig. 3*E*,*F*) ($n = 13$). Taking into account a release probability of 0.87, the amplitude of the isolated synaptic voltage response in these spines is estimated to be ~13 mV. We observed no significant influence of spine neck length (1.3 ± 0.1 μm) or dendritic location (37–140 μm from the soma) on the amplitude of the synaptic voltage isolated in the spine head (data not shown).

The majority of spines (57 of 70) had an isolated calcium signal and a large change in fluorescence in response to bAPs (average: 5.8 ± 0.3% $\Delta F/F$), but no clear fluorescence response during synaptic stimulation (response <2.5 times the SD of the noise) (see Materials and Methods). Although individual spines did not show clear responses to synaptic stimulation, when averaged together the EPSP in these spines was discernible and only slightly larger than that observed in the parent dendrite (average spine response: 2.0 mV; $n = 57$). It seems likely that these responses are largely attributable to activation of neighboring inputs rather than the imaged spine. Further analysis of these responses revealed that despite no obvious changes in spine morphology, or a change in the voltage response during back-propagating APs, we detected significant rundown of synaptic responses in these spines (supplemental Fig. 3, available at www.jneurosci.org as supplemental material). As a result, we do not include these responses in subsequent analysis.

Contribution of voltage-activated channels to the spine synaptic signal

In addition to containing glutamatergic receptors (AMPA and NMDA), spines contain various voltage-activated channels, including calcium channels (Sabatini and Svoboda, 2000; Bloodgood and Sabatini, 2007) and possibly sodium channels (Tsay and Yuste, 2002; Araya et al., 2007). An open question is whether the voltage change in the spine head during the synaptic response can be boosted via activating voltage-activated channels (Miller et al., 1985; Perkel and Perkel, 1985; Segev and Rall, 1988; Araya et al., 2007). To test this, active spines were sequentially stimulated at rest (Fig. 4*A*) and at hyperpolarized potentials (Fig. 4*B*). Hyperpolarization will increase the driving force for current flow through glutamatergic receptors, boosting the size of the primarily AMPA-mediated voltage response. Conversely, hyperpolarization will decrease the likelihood that the synaptic voltage reaches threshold to activate voltage-activated sodium and calcium channels, reducing their potential contribution to the synaptic response. These effects would be expected to lead to opposite changes in the amplitude of the synaptic response during hyperpolarization. Comparison of the spine response at resting membrane potentials (21.1 ± 3.8 mV; $n = 13$) with that at hyperpolarized membrane potentials (36.6 ± 2.8 mV; $n = 13$) illustrates that the spine response is significantly increased by hyperpolarization (Fig. 4*C*). The isolated spine response in these experiments increased from 13.2 ± 2.2 mV at the resting membrane potential to 19.2 ± 2.2 mV during hyperpolarization ($p <$

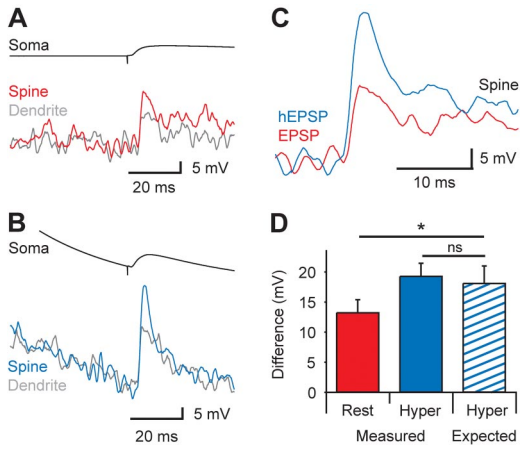

Figure 4. Voltage-activated channels do not boost synaptic responses in spines. ***A***, ***B***, Average ($n = 13$) response to synaptic stimulation recorded at the soma (top) and in spines (bottom) at rest (***A***; −72 mV at the soma) and during hyperpolarizing current injection (***B***; −106 mV). ***C***, Comparison of the average synaptic fluorescence response in spines at rest (EPSP, red) and at hyperpolarized membrane potentials (hEPSP, blue). ***D***, Histogram of the average isolated spine response during synaptic stimulation at rest (red) and hyperpolarized membrane potentials (blue), together with the expected response at the hyperpolarized membrane potential (blue striped) based purely on the increase in driving force during hyperpolarization ($n = 13$). Data show mean ± SEM. ns, Nonsignificant. *$p < 0.05$.

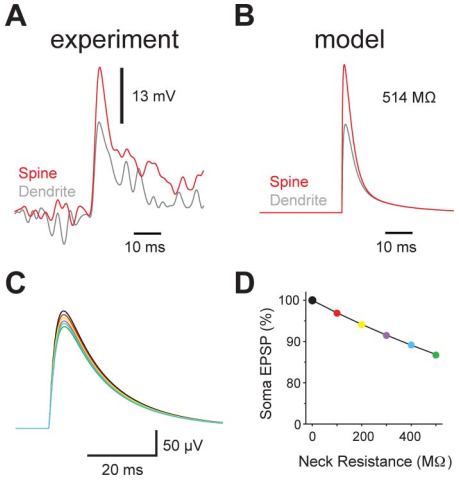

Figure 5. Spine neck resistance and its impact on synaptic strength. ***A***, Superaverage of the synaptic voltage response in spines (red) and parent dendrites (gray) for spines with a discernible synaptic response at rest (top; $n = 13$). The difference in the spine and dendrite synaptic voltage responses is indicated. ***B***, Simulation of experimentally observed voltage changes during synaptic stimulation for a spine located 80 μm from the soma in a model (see Materials and Methods). Activation of spines other than the one imaged was achieved by simultaneous activation of synaptic inputs located on the same dendrite. The spine neck resistance is indicated. ***C***, Simulation of EPSPs at the soma in response to synaptic input (500 pS) onto a spine located 80 μm from the soma for spine neck resistances from 0 MΩ (black) to 500 MΩ (green). ***D***, Plot of simulated somatic EPSP amplitude (% of maximum) versus spine neck resistance during synaptic input (500 pS) onto a spine located 80 μm from the soma with spine neck resistances from 0 MΩ (black) to 500 MΩ (green). These data suggest that modulation of spine neck resistance over the physiological range reduces synaptic strength by <15%. Points are color coded to match the traces in ***C***.

0.05, $n = 13$). Based on the assumption that this increase is attributable solely to the change in driving force, the amplitude of the spine response at the hyperpolarized membrane potential can be estimated from the amplitude of the response at the resting membrane potential (−74 ± 1 mV). This analysis revealed that there was no significant difference between the measured voltage in active spines at hyperpolarized membrane potentials and that predicted from the change in driving force (Fig. 4*D*) (predicted: 18.0 ± 2.9 mV; $p > 0.05$; $n = 13$), indicating that voltage-activated channels are unlikely to significantly contribute to the synaptic voltage response in dendritic spines. Consistent with this idea, there was no significant difference in the rise-time (2.2 ± 0.7 vs 2.2 ± 0.5 ms) or half-width (3.0 ± 0.5 vs 3.4 ± 0.3 ms) of spine responses at rest and hyperpolarized membrane potentials. Furthermore, subthreshold depolarization (average: 9.7 ± 0.7 mV; 150 ms; $n = 8$) did not increase the amplitude of synaptic spine responses, inconsistent with boosting by voltage-activated channels. These findings are consistent with theoretical studies (Miller et al., 1985; Perkel and Perkel, 1985; Segev and Rall, 1988), which indicate that regenerative responses in spines require densities of voltage-activated sodium channels >100-fold higher than experimental estimates in dendrites of cortical pyramidal neurons (Stuart and Sakmann, 1994).

Spine neck resistance

It has long been speculated that modulation of spine neck resistance could act to regulate synaptic strength (Rall, 1970). Modulation of spine neck resistance alters the amplitude of the synaptic response in the spine, influencing the driving force for synaptic current flow and therefore the amplitude of the synaptic voltage change in the parent dendrite and soma. The higher the spine neck resistance, the larger the synaptic voltage change in the spine head, and the greater the reduction in driving force for synaptic current flow. Hence, high spine neck resistances lead to smaller synaptic voltage changes at the soma. To calculate spine neck resistance and its impact on the amplitude of the synaptic response at the soma, we simulated spine and parent dendrite synaptic responses using a morphologically realistic model of a layer 5 pyramidal neuron.

We used data from spines with a clear synaptic response at the resting membrane potential (Fig. 5*A*; same data as in Fig. 3*D*, bottom). These data represent the largest spine responses observed. Because these larger synaptic voltage responses presumably arise because of higher spine neck resistances, these data can be used to put an upper bound on spine neck resistance. Simulation of these synaptic responses revealed a spine neck resistance of ~500 MΩ (Fig. 5*B*). We next performed simulations to investigate how spine neck resistances up to this value influence somatic EPSP amplitude (Fig. 5*C*). These simulations showed that increasing spine neck resistance up to 500 MΩ leads to reductions in somatic EPSP amplitude of <15% (Fig. 5*D*).

Discussion

Although the role of dendritic spines has been a source of controversy ever since their description by Cajal over a century ago, their importance in neuronal signaling has never been questioned: the vast majority of excitatory synaptic input in many brain regions is made directly onto dendritic spines, which presumably play an essential role in synaptic transmission and plasticity. Although it is clear that spines can act as biochemical compartments (Muller and Connor, 1991; Yuste and Denk, 1995), whether they also act as electrical compartments is unclear. We provide the first direct estimates of the voltage experienced by dendritic spines during synaptic activation. These data indicate that synaptic responses in spines range from a few millivolts up to ~20 mV, and that the spine neck resistance can lead to electrical compartmentalization in some spines. Furthermore, we estimate an upper bound of spine neck resistance of ~500 MΩ. By altering spine neck resistance over the range observed in our experiments,

we show that in most spines it is unlikely the spine neck will act as a physical device to significantly modulate synaptic strength. Finally, we show that bAPs effectively invade dendritic spines without voltage loss (Nuriya et al., 2006), which is presumably critical for their role as a retrograde messenger during spike-timing dependent synaptic plasticity (Magee and Johnston, 1997; Markram et al., 1997; Koester and Sakmann, 1998).

The experiments described here were performed on large spines with a high release probability. Electrical compartmentalization and the capacity for spine neck resistance to modulate synaptic strength may be greater in spines with different morphologies (Crick, 1982; Koch and Poggio, 1983). Thin filopodia-like spines, which were less accessible to voltage imaging because of their small surface area, may show even greater electrical compartmentalization, as recently reported by Araya et al. (2006), and consequently an increased capacity to modulate synaptic strength. In addition, it should be noted that the experiments described here were performed *in vitro* at room temperature to increase temporal resolution by slowing down the voltage response. The extent of electrical compartmentalization may differ at physiological temperatures and *in vivo*.

Imaged spines in our study were located on basal dendrites of cortical layer 5 pyramidal neurons. The question arises whether the responses reported here can be generalized to other dendritic areas. Because the spine head encounters the impedance from both the spine neck and dendrite, spines on smaller dendrites with higher input resistances would be expected to have larger voltage responses to the same synaptic input (Rall and Rinzel, 1973). As a consequence, one would expect the extent of electrical compartmentalization, as well as the absolute magnitude of synaptic spine responses, will depend on both the overall dendritic morphology as well as the specific location of spines in the dendritic tree.

The purpose of voltage-activated channels in spines

What is the purpose of voltage-activated channels in spines? One possibility is that voltage-activated sodium channels in dendritic spines are required for supporting active propagation of APs into the dendritic tree (Tsay and Yuste, 2002). In addition, voltage-activated sodium and calcium channels in spines are likely to be activated by, and contribute to, dendritic spikes. The voltage change in spines during bAPs and dendritic spikes will enhance the removal of the voltage-dependent magnesium block of NMDA channels, and thereby is likely to play a role in the induction of some forms of synaptic plasticity (Kampa et al., 2007; Sjöström et al., 2008). Effective propagation of bAPs and dendritic spikes into dendritic spines is required for all these processes. Consistent with this, we observed that bAPs invade dendritic spines without voltage loss (Fig. 2).

The question remains to what extent voltage-activated channels are activated by synaptic inputs. Previous data suggest that voltage-activated calcium channels in spines can be activated by artificial EPSPs generated by glutamate uncaging (Bloodgood and Sabatini, 2007), which counter-intuitively decreased (rather than increased) the amplitude of voltage responses. It was concluded that this occurs because of activation of calcium-activated potassium channels in spines (Bloodgood and Sabatini, 2007), which have recently been shown to modulate synaptic NMDA receptor activation (Faber et al., 2005; Ngo-Anh et al., 2005). With respect to voltage-activated sodium channels the situation is more complicated, with one study using glutamate uncaging arguing there is little impact of voltage-activated sodium channels in spines on the amplitude of voltage response (Bloodgood and Sabatini, 2007), whereas another study using the same technique has proposed that voltage-activated sodium channels in spines can boost the voltage response observed at the soma (Araya et al., 2007). In contrast, changes in resting membrane potential influenced the amplitude of synaptic responses in spines in a way that was consistent with a change in the driving force for current flow through AMPA receptor channels, rather than via a change the activation of voltage-activated channels. Presumably this is the case for two reasons. First, the voltage response during synaptic input is typically too small to significantly activate voltage-activated channels in spines (see Fig. 3*F*), and second, the density of active voltage-activated channels in spines is likely to be too low to generate significant boosting of the synaptic voltage response in the spine head. As noted above, previous theoretical studies indicate that regenerative responses in spines require densities of voltage-activated sodium channels >100-fold higher than experimental estimates in dendrites of cortical pyramidal neurons (Miller et al., 1985; Perkel and Perkel, 1985; Segev and Rall, 1988).

Spine neck resistance estimates compared with previous studies

We provide an upper bound of spine neck resistance of approximately 500 MΩ based on modeling spine and parent dendrite voltage responses (Fig. 5*A*,*B*). This estimate encompasses previous estimates of spine neck resistance based on reconstructions from electron microscopy (Harris and Stevens, 1989) (CA1 pyramidal neurons: 0.9–411 MΩ; cerebellar Purkinje cells: 2.6–80 MΩ), and is also similar to, albeit somewhat higher than, spine neck resistance estimates calculated by dye diffusion (Svoboda et al., 1996) (CA1 pyramidal neurons: 4–150 MΩ), although a more recent study using this technique has suggested that some spines have spine neck resistances that can approach 1 GΩ (Bloodgood and Sabatini, 2005). Our estimate is also similar to that recently obtained based on modeling experimental observations on calcium influx into dendritic spines via NMDA receptors (Grunditz et al., 2008). Finally, simulations of spine neck resistance of up to 500 MΩ required spine neck diameters from ~0.2 to 0.05 μm (assuming a spine neck length of 1 μm). These values line up well with previous evidence in CA1 pyramidal neurons, which indicate spine neck diameters range from 0.46 to 0.038 μm (Harris and Stevens, 1989). In contrast, a recent study has proposed that steady-state voltage attenuation across the spine neck can approach 50% (Araya et al., 2006). This would require spine neck resistances on the order of 1000 GΩ and an internal spine neck diameter of <2 nm (assuming a spine neck length of 1 μm and internal resistance of 105 Ωcm) (G. J. Stuart, unpublished observations), which seems unrealistic.

Implications for synaptic plasticity

It has long been proposed that spine morphology could directly alter synaptic strength (Chang, 1952; Rall and Rinzel, 1973). This can occur as higher spine neck resistances, associated with longer, thinner spine necks, would be expected to increase the voltage change in the spine head during a given synaptic input, reducing the driving force for synaptic current flow (Koch and Zador, 1993). This idea is consistent with recent studies that report a negative correlation between spine neck length and the peak amplitude of the somatic voltage change during glutamate uncaging onto dendritic spines (Araya et al., 2006, 2007). Such a correlation was not observed in our study. This may indicate that factors other than purely spine neck length can influence the amplitude of synaptic responses in the spine head. One possibility is that

spines with longer necks have reduced numbers of AMPA receptors, as has been recently reported by a number of studies (Ashby et al., 2006; Korkotian and Segal, 2006, 2007).

In conclusion, our observations indicate that there are likely to be significant differences in spine neck resistance across different spines, with spine neck resistance ranging up to ~500 MΩ. Even our highest estimates of spine neck resistances are likely to be too low to significantly influence the amplitude of synaptic potentials at the soma, with the highest spine neck resistances leading to reductions in somatic EPSP amplitude of <15%. These observations suggest that for the majority of spines, the spine neck is unlikely to act as a physical device to modulate synaptic strength.

References

Araya R, Jiang J, Eisenthal KB, Yuste R (2006) The spine neck filters membrane potentials. Proc Natl Acad Sci U S A 103:17961–17966.

Araya R, Nikolenko V, Eisenthal KB, Yuste R (2007) Sodium channels amplify spine potentials. Proc Natl Acad Sci U S A 104:12347–12352.

Ashby MC, Maier SR, Nishimune A, Henley JM (2006) Lateral diffusion drives constitutive exchange of AMPA receptors at dendritic spines and is regulated by spine morphology. J Neurosci 26:7046–7055.

Bekkers JM, Stevens CF (1990) Presynaptic mechanism for long-term potentiation in the hippocampus. Nature 346:724–729.

Bloodgood BL, Sabatini BL (2005) Neuronal activity regulates diffusion across the neck of dendritic spines. Science 310:866–869.

Bloodgood BL, Sabatini BL (2007) Nonlinear regulation of unitary synaptic signals by CaV(2.3) voltage-sensitive calcium channels located in dendritic spines. Neuron 53:249–260.

Chang HT (1952) Cortical neurons with particular reference to the apical dendrites. Cold Spring Harb Symp Quant Biol 17:189–202.

Crick F (1982) Do dendritic spines twitch? Trends Neurosci 5:44–46.

Denk W, Sugimori M, Llinás R (1995) Two types of calcium response limited to single spines in cerebellar Purkinje cells. Proc Natl Acad Sci U S A 92:8279–8282.

Djurisic M, Antic S, Chen WR, Zecevic D (2004) Voltage imaging from dendrites of mitral cells: EPSP attenuation and spike trigger zones. J Neurosci 24:6703–6714.

Faber ES, Delaney AJ, Sah P (2005) SK channels regulate excitatory synaptic transmission and plasticity in the lateral amygdala. Nat Neurosci 8:635–641.

Grunditz A, Holbro N, Tian L, Zuo Y, Oertner TG (2008) Spine neck plasticity controls postsynaptic calcium signals through electrical compartmentalization. J Neurosci 28:13457–13466.

Harris KM, Stevens JK (1989) Dendritic spines of CA 1 pyramidal cells in the rat hippocampus: serial electron microscopy with reference to their biophysical characteristics. J Neurosci 9:2982–2997.

Häusser M, Roth A (1997) Estimating the time course of the excitatory synaptic conductance in neocortical pyramidal cells using a novel voltage jump method. J Neurosci 17:7606–7625.

Hines ML, Carnevale NT (1997) The NEURON simulation environment. Neural Comput 9:1179–1209.

Kampa BM, Letzkus JJ, Stuart GJ (2007) Dendritic mechanisms controlling spike-timing-dependent synaptic plasticity. Trends Neurosci 30:456–463.

Koch C, Poggio T (1983) A theoretical analysis of electrical properties of spines. Proc R Soc Lond B Biol Sci 218:455–477.

Koch C, Zador A (1993) The function of dendritic spines: devices subserving biochemical rather than electrical compartmentalization. J Neurosci 13:413–422.

Koester HJ, Sakmann B (1998) Calcium dynamics in single spines during coincident pre- and postsynaptic activity depend on relative timing of back-propagating action potentials and subthreshold excitatory postsynaptic potentials. Proc Natl Acad Sci U S A 95:9596–9601.

Korkotian E, Segal M (2006) Spatially confined diffusion of calcium in dendrites of hippocampal neurons revealed by flash photolysis of caged calcium. Cell Calcium 40:441–449.

Korkotian E, Segal M (2007) Morphological constraints on calcium dependent glutamate receptor trafficking into individual dendritic spine. Cell Calcium 42:41–57.

Magee JC, Johnston D (1997) A synaptically controlled, associative signal for Hebbian plasticity in hippocampal neurons. Science 275:209–213.

Markram H, Lübke J, Frotscher M, Sakmann B (1997) Regulation of synaptic efficacy by coincidence of postsynaptic APs and EPSPs. Science 275:213–215.

Miller JP, Rall W, Rinzel J (1985) Synaptic amplification by active membrane in dendritic spines. Brain Res 325:325–330.

Müller W, Connor JA (1991) Dendritic spines as individual neuronal compartments for synaptic Ca2+ responses. Nature 354:73–76.

Nevian T, Larkum ME, Polsky A, Schiller J (2007) Properties of basal dendrites of layer 5 pyramidal neurons: a direct patch-clamp recording study. Nat Neurosci 10:206–214.

Ngo-Anh TJ, Bloodgood BL, Lin M, Sabatini BL, Maylie J, Adelman JP (2005) SK channels and NMDA receptors form a Ca^{2+}-mediated feedback loop in dendritic spines. Nat Neurosci 8:642–649.

Nuriya M, Jiang J, Nemet B, Eisenthal KB, Yuste R (2006) Imaging membrane potential in dendritic spines. Proc Natl Acad Sci U S A 103:786–790.

Perkel DH, Perkel DJ (1985) Dendritic spines: role of active membrane in modulating synaptic efficacy. Brain Res 325:331–335.

Rall W (1970) Cable properties of dendrites and effects of synapse location. In: Excitatory synaptic mechanisms (Andersen P, Jansen JKS, eds), pp 175–187. Oslo: Universitetsforlaget.

Rall W, Rinzel J (1973) Branch input resistance and steady attenuation for input to one branch of a dendritic neuron model. Biophys J 13:648–687.

Rose CR, Konnerth A (2001) NMDA receptor-mediated Na^+ signals in spines and dendrites. J Neurosci 21:4207–4214.

Rose CR, Kovalchuk Y, Eilers J, Konnerth A (1999) Two-photon Na^+ imaging in spines and fine dendrites of central neurons. Pflugers Arch 439:201–207.

Sabatini BL, Svoboda K (2000) Analysis of calcium channels in single spines using optical fluctuation analysis. Nature 408:589–593.

Sabatini BL, Oertner TG, Svoboda K (2002) The life cycle of Ca^{2+} ions in dendritic spines. Neuron 33:439–452.

Segev I, Rall W (1988) Computational study of an excitable dendritic spine. J Neurophysiol 60:499–523.

Sjöström PJ, Rancz EA, Roth A, Häusser M (2008) Dendritic excitability and synaptic plasticity. Physiol Rev 88:769–840.

Stuart G, Spruston N (1998) Determinants of voltage attenuation in neocortical pyramidal neuron dendrites. J Neurosci 18:3501–3510.

Stuart GJ, Palmer LM (2006) Imaging membrane potential in dendrites and axons of single neurons. Pflugers Arch 453:403–410.

Stuart GJ, Sakmann B (1994) Active propagation of somatic action potentials into neocortical pyramidal cell dendrites. Nature 367:69–72.

Stuart GJ, Dodt HU, Sakmann B (1993) Patch-clamp recordings from the soma and dendrites of neurons in brain slices using infrared video microscopy. Pflugers Arch 423:511–518.

Svoboda K, Tank DW, Denk W (1996) Direct measurement of coupling between dendritic spines and shafts. Science 272:716–719.

Tsay D, Yuste R (2002) Role of dendritic spines in action potential backpropagation: a numerical simulation study. J Neurophysiol 88:2834–2845.

Yuste R, Denk W (1995) Dendritic spines as basic functional units of neuronal integration. Nature 375:682–684.